Preprints of the 19th World Congress
The International Federation of Automatic Control
Cape Town, South Africa. August 24-29, 2014

Fault Diagnosis of Advanced Wind Turbine Benchmark using Interval-based ARRs and Observers

Hector Sanchez * **Teresa Escobet** * **Vicenç Puig** *

* *Automatic Control Department, Technical University of Catalonia (UPC), Rambla Sant Nebridi 22, 08222 Terrassa, Spain; (e-mail:{hector.eloy.sanchez, teresa.escobet, vicenc.puig}@upc.edu).*

Abstract:
In this paper, the problem of the fault diagnosis of an advanced wind turbine benchmark will be addressed using analytical redundant relations (ARRs) and observers that considers uncertainty in a bounded context, using the so-called interval approach. The fault detection test is based on checking the consistency between the measurements and the model by finding if the formers are inside the interval bounds provided by the interval model. In case a fault is detected, using the theoretical fault signature matrix against the full set of residuals available on-line, the fault is isolated. Two fault isolation schemes are compared. One based in the classical column matching and the other one using the row-reasoning inspired in the DX fault diagnosis approach. Finally, the proposed approach will be tested using the advanced wind turbine benchmark proposed in the literature.

1. INTRODUCTION

Wind turbines have become an important source of renewable power generation in the last years. A major issue with wind turbines systems specially those located offshore, is the relatively high cost of operation and maintenance (OM). Also, poor reliability directly reduces availability of wind power due to the turbine downtime. Condition monitoring and fault diagnosis of wind turbines has thus greater benefit for such situations.

Due to the great interest in fault diagnosis of wind turbines coming from the industry and academia, a first benchmark paper and competition about fault detection and isolation of wind turbines was presented in [Odgaard and Stoustrup, 2013]. After the announcement of results of the first benchmark, a second challenge was presented in [Odgaard and Johnson, 2013]. This second challenge differed from the previous one in several ways: wind turbine is modeled in FAST simulator [Jonkman et al., 2005], differing from the first benchmark in which all the subsystem models were provided. This means that a higher-fidelity, more detailed, aerodynamic, structural and realistic wind turbine model was used, requiring more sophisticated fault detection and fault-tolerant control tools and likely making the results of greater applicability to the wind industry. This higher-fidelity model also allows the use of more realistic wind inputs that vary spatially across the rotor plane in addition to temporally. Also, the fault scenarios were updated and additional information detailing their relevance was provided.

Fault detection and isolation methods can be classified as either model or data based. In this paper, a model-based approach that combines the use of analytical redundancy relations (ARRs) and observers is used. Uncertainty in parameters and noise is modeled using an unknown but bounded approach. This leads to formulate the fault detection test based on checking if the measurements fall inside the estimated output interval obtained from the mathematical model of the wind turbine. Finally, results obtained in the advanced wind turbine benchmark are presented.

The structure of the paper is the following: In Section 2, the ARRs obtained from the available measurements and the fault diagnosis model are presented. Section 3 presents how parametric uncertainty is estimated. The fault diagnosis scheme is presented in Section 4. The results obtained with the proposed approach applied to the advance wind turbine benchmark are summarized in Section 5. Conclusions are presented in Section 6.

2. ARR GENERATION

The overall wind turbine system model of the advanced wind turbine benchmark is divided into appropriate submodels suitable of being modeled separately to perform fault diagnosis. The different submodels collected from the literature are used for generating the ARRs. These are the Blade and Pitch model, Power Subsystem model, Drive train model and Blade Root Moment model. The interaction between these subsystems is illustrated in (Fig. 1).

The design of the fault diagnosis system is based on deriving a set of ARRs by combining the model equations with the available sensors.

ARRs are defined as relations between known variables and can be derived combining the measurement model (known variables) with the system model (unknown variables). Combining the model equations with the available sensors described in the wind turbine benchmark [Odgaard and Johnson, 2013], by means of the structural analysis

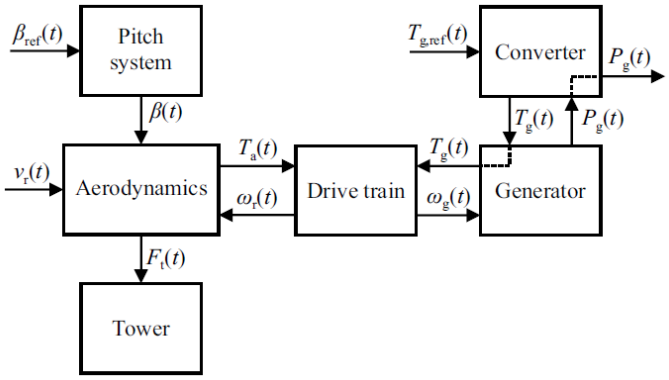

Fig. 1. Subsystems models interaction of the wind turbine system model.

approach [Blanke et al., 2006] the following set of dynamic and static ARRs is presented below.

2.1 Static ARRs

ARR 1 is obtained directly from the model presented in Odgaard and Stoustrup [2013]

$$P_{\rm gm}(t) = \eta_{\rm g}\omega_{\rm gm}(t)T_{\rm gm}(t) \quad (1)$$

because the power generated $P_{\rm gm}(t)$, the rotor speed $\omega_{\rm gm}$ and the generator torque $T_{\rm gm}(t)$ are all measured variables.

ARRs 2, 3 and 4 are obtained from the blade root moment model presented in [Markou et al., 2002]. During the simulation tests performed with FAST simulator, some problems were found with this model and the behavior did not correspond to the one observed in the simulations. After observing this phenomenon in the blade root moment behavior and considering the influence of the wind speed and blades pitch angle on this variable, an experimental model was proposed to be used. This experimental model is based on the mean values of the blade root moment and pitch angle signals in steady state. Several tests with different constant wind speeds and therefore different pitch angles were performed. A relation between the different pitch angles and the mean value of the blade root moment in steady state was found. As it can be seen in Figure (2) a first, second and third order polynomials were considered to represent the mean blade root moment as function of the pitch angle.

Finally, the proposed model for the blade root moment dynamics was the third order blade root moment mean model:

$$\bar{M}_{B,i,m(t)} = a_3\bar{\beta}_{i,m}(t)^3 + a_2\bar{\beta}_{i,m}(t)^2 + a_1\bar{\beta}_{i,m}(t) + a_0 \quad (2)$$

where: $\bar{M}_{B,i}(t)$ is the blade root moment and $\bar{\beta}_i$ is the pitch angle on blade i. The values of the coefficients α_i for blade root moment mean models for each one of the blades corresponding to experiments of winds higher than 12 m/s, are shown in Table 1.

ARR 9 (eq. 3) and *ARR 12* (eq. 4) were derived considering the steady state behavior of the drive train model proposed in [Esbensen et al., 2009]. A relation between $\omega_{g,m}(t)$ and $T_{g,m}(t)$

$$B_g\omega_{g,m}(t) = -T_{g,m}(t) + K \quad (3)$$

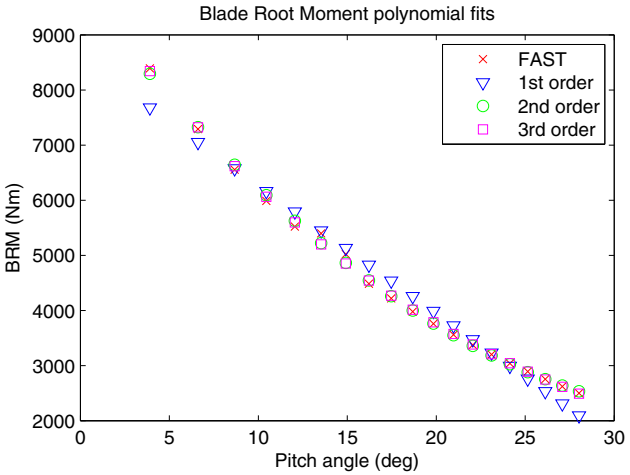

Fig. 2. Estimated Blade Root Moments models

Table 1. Blade Root Moment Mean Model Coefficients

Mean BRM model	α_3	α_2	α_1	α_0
$\bar{M}_{B,1(t)}$	-0.0778	9.3204	-469.4313	10038
$\bar{M}_{B,2(t)}$	-0.0777	9.3159	-469.3210	10037
$\bar{M}_{B,3(t)}$	-0.0776	9.3228	-469.6690	10040

where the constant K is the torsion angle in steady state, as well a relation between $\omega_{g,m}(t)$ and $\omega_{r,m}(t)$ through N_g can be established as follows

$$\omega_{rm}(t) - \frac{1}{N_g}\omega_{gm}(t) = 0 \quad (4)$$

where: B_g is the viscous friction of the high-speed shaft, N_g is the gearbox ratio, $T_{g,m}(t)$ is the generator torque, $\omega_{g,m}(t)$ and $\omega_{r,m}(t)$ are the measured generator and rotor speed, respectively.

2.2 Dynamic ARRs

ARR 5 is obtained from the generator/converter model in [Esbensen et al., 2009] as follows

$$\tau_{\rm g}\frac{dT_{gm}(t)}{dt} + T_{gm}(t) = T_{\rm g,ref}(t) \quad (5)$$

where $T_{gm}(t)$ and $T_{\rm g,ref}(t)$ are the measured and reference torque, respectively.

ARRs 6, 7 and *8* are the ARRs for the pitch subsystems derived from the model proposed in [Odgaard and Stoustrup, 2013] according to

$$\frac{d^2\beta_{i,m}(t)}{dt^2} + 2\zeta\omega_n\frac{d\beta_{i,m}(t)}{dt} + \omega_n^2\beta_{i,m}(t) = \omega_n^2\beta_{ref}(t) \quad (6)$$

where $\beta_{i,m}$ is the pitch angle in the i_{th} blade and the reference is β_r.

Using the input/output equations of the drive train model presented in [Esbensen et al., 2009] with the dynamics of the torsion angle neglected because there is no sensor available for this variable in the benchmark, ARR 10 (eq. 7) and ARR 11 (eq. 8) are obtained

$$f_1\left(\dot{\omega}_{rm}(t), \omega_{rm}(t), T_{a*}(t), T_{gm}(t)\right) = 0 \quad (7)$$

$$f_2\left(\dot{\omega}_{gm}(t), \omega_{gm}(t), T_{a*}(t), T_{gm}(t)\right) = 0 \quad (8)$$

where the aerodynamic torque $T_{a*}(t)$ can be estimated because it is function of known variables through the following expression

$$T_{a*}(t) = f\left(\omega_{rm}(t), v_m(t), \beta_m(t)\right) \quad (9)$$

3. MODELS FOR FAULT DETECTION

3.1 Static and dynamic models

Previous ARRs will be used to create residuals to detect and isolate faults. These residuals will be generated in order to check the consistency between the observed and the predicted process behavior. Looking at the obtained ARRs, they can be divided in two groups: static and dynamic.

The generation of residuals is straightforward in case of static ARRs since they follow directly from the mathematical expressions. On the other hand, in case of dynamic ARRs several options for generating residuals are possible ranging from parity equations to observers. In this paper, residuals generated using observers for dynamic ARRs have been preferred because the enhanced fault detection performance achieved after their application to the advanced wind turbine benchmark.

The model of each dynamic ARRs is rewritten in observer canonical form as follows:

$$x(k+1) = A(\tilde{\theta})x(k) + B(\tilde{\theta})u(k) \quad (10)$$

$$y(k) = C(\tilde{\theta})x(k) + \tilde{v}(k) \quad (11)$$

where $u(k) \in \mathbb{R}^{n_u}$ is the system input, $y(k) \in \mathbb{R}^{n_y}$ is the system output, with $x(k) \in \mathbb{R}^{n_x}$ is the state-space vector, $\tilde{v}(k) \in \mathbb{R}^{n_y}$ is the output noise that is assumed to be bounded $|\tilde{v}_i(k)| < \sigma_i$, with $i = 1, \ldots, n_y$, $A(\tilde{\theta})$, $B(\tilde{\theta})$, $C(\tilde{\theta})$, are matrices of appropriate dimensions where $\tilde{\theta} \in \mathbb{R}^{n_\theta}$ is the parameter vector. Uncertainty in the parameters is considered as follows

$$\theta \in \Theta = \left\{\theta \in \mathbb{R}^{n_\theta} \mid \underline{\theta}_i \leq \theta_i \leq \bar{\theta}_i, i = 1, \ldots, n_\theta\right\} \quad (12)$$

Then, from the dynamic ARR expressed in state space form (10)-(11), a interval linear observer with Luenberger structure is considered as follows:

$$\begin{aligned}\hat{x}(k+1,\theta) &= \left(A(\theta) - LC(\theta)\right)\hat{x}(k,\theta) + B(\theta)u(k) + Ly(k)\\ &= A_0(\theta)\hat{x}(k,\theta) + B(\theta)u(k) + Ly(k) \quad (13)\\ \hat{y}(k,\theta) &= C(\theta)\hat{x}(k,\theta)\end{aligned}$$

where $\hat{x}(k,\theta)$ is the estimated system state vector, $\hat{y}(k,\theta)$ is the estimated system output vector and $A_0(\theta) = A(\theta) - LC(\theta)$ is the observer matrix. The observer gain matrix $L \in \mathbb{R}^{n_x \times n_y}$ is designed to stabilize the matrix $A_0(\theta)$ and to guarantee a desired performance regarding fault detection for all $\theta \in \Theta$ using the LMI pole placement approach [Chilali et al., 1996].

The input/output form of the observer (13) is expressed as follows:

$$\hat{y}(k,\theta) = G(q^{-1},\theta)u(k) + H(q^{-1},\theta)y(k) \quad (14)$$

with:

$$G(q^{-1},\theta) = C(\theta)(qI - A_0(\theta))^{-1}B(\theta) \quad (15)$$

$$H(q^{-1},\theta) = C(\theta)(qI - A_0(\theta))^{-1}L \quad (16)$$

The effect of the uncertain parameters θ on the observer temporal response $\hat{y}(k,\theta)$ will be bounded using an interval satisfying:

$$\hat{y}(k,\theta) \in \left[\underline{\hat{y}}(k), \overline{\hat{y}}(k)\right] \quad (17)$$

Such interval can be computed independently for each output $i = 1, \ldots, n_y$, neglecting couplings among outputs, as follows:

$$\underline{\hat{y}_i}(k) = \min_{\theta\in\Theta} \hat{y}_i(k,\theta) \quad \text{and} \quad \overline{\hat{y}}_i(k) = \max_{\theta\in\Theta} \hat{y}_i(k,\theta) \quad (18)$$

subject to the observer equations given by (14). The bounds shown in (18) can be determined using the zonotope approach presented in [Puig et al., 2013].

Finally, taking into account that the additive noise in the system (11) is bounded, the following condition should be satisfied

$$y_i(k) \in \left[\underline{\hat{y}_i}(k) - \sigma_i, \overline{\hat{y}_i}(k) + \sigma_i\right] \; i = 1, \ldots, n_y \quad (19)$$

in a non-faulty scenario.

3.2 Parameter uncertainty estimation

One of the key points in passive robust model based fault detection is how models and their uncertainty bounds are obtained. Assuming that the measured variables are corrupted by additive noises with known statistical distributions and that the model structure is known, a parameter estimation algorithm will provide nominal values for the parameters together with descriptions of the associated uncertainty in terms of the covariance matrix or confidence regions for a given probability level. However, this type of approaches cannot be applied when measurement errors are described as unknown but bounded values and/or modeling errors exist. The problem of bounding the model uncertainty has been mainly stated in many references coming from the robust control field.

The methodology *bounded-error* or *set-membership estimation* [Milanese et al., 1996] assumes the bounded but unknown description of the noise and parametric uncertainty, which produces a set of parameters consistent with the selected model structure and the pre-specified noise bounds. This approach is used for estimating parametric uncertainty of the interval observers in (13). The goal of the parameter estimation algorithm is to characterize the parameter set Θ (here a box) consistent with the data collected in a fault-free scenario. Given N measurements of system inputs $y(k)$ and outputs $u(k)$ from a scenario free of faults and rich enough from the identifiability point of view, the parameters tolerance α, and a nominal model described by a vector θ_n obtained using a standard least-square parameter estimation algorithm, the uncertain parameter estimation algorithm proceeds by solving the optimization problem (20).

$$\begin{aligned}&\min\ \alpha\\ &\text{subject to :}\\ &y_i(k) \in \left[\underline{\hat{y}}_i(k) - \sigma_i, \overline{\hat{y}}_i(k) + \sigma_i\right] \quad i = 1, ..., n_y \quad k = 1, ..., N\\ &\underline{\hat{y}}_i(k) = \min_{\theta\in\Theta} \hat{y}_i(k,\theta) \quad i = 1, ..., n_y \quad k = 1, ..., N\\ &\overline{\hat{y}}_i(k) = \max_{\theta\in\Theta} \hat{y}_i(k,\theta) \quad i = 1, ..., n_y \quad k = 1, ..., N\\ &\hat{y}(k,\theta) = G(q^{-1},\theta)u(k) + H(q^{-1},\theta)y(k) \quad k = 1, ..., N\\ &\Theta = [\theta_n(1-\alpha), \theta_n(1+\alpha)]\end{aligned} \quad (20)$$

Regarding the uncertain variables that appear in (13), it is assumed that a priori theoretical or practical considerations allow to obtain useful intervals associated to measurement noises (19), leading to an estimation of the noise bound σ. A similar algorithm can be used for the static ARRs.

4. FAULT DIAGNOSIS APPROACH

4.1 Fault Detection

Fault detection is based on generating a nominal residual comparing the measurements of physical system variables $y(k)$ with their estimation $\hat{y}(k)$ provided by the observer (13):

$$r(k) = y(k) - \hat{y}(k, \theta_n) \tag{21}$$

where $r(k) \in \mathbb{R}^{n_y}$ is the residual set and θ_n the nominal parameters. The form of the nominal residual generator, obtained using (14), is:

$$r(k) = \left(I - H(q^{-1}, \theta_n)\right) y(k) - G(q^{-1}, \theta_n) u(k) \tag{22}$$

that has been derived taking into account the input/output form of the observer.

When considering model uncertainty located in parameters, the residual generated by (21) will not be zero, even in a non-faulty scenario. To cope with the parameter uncertainty effect, a passive robust approach based on adaptive thresholding can be used [Puig et al., 2006]. Thus, using this passive approach, the effect of parameter uncertainty in the components $r_i(k)$ of residual $r(k)$ (associated to each system output $y_i(k)$) is bounded by the interval [Puig et al., 2006]:

$$r_i(k) \in [\underline{r}_i(k) - \sigma_i, \overline{r}_i(k) + \sigma_i] \quad i = 1, ..., n_y \tag{23}$$

where:

$$\underline{r}_i(k) = \underline{\hat{y}}_i(k) - \hat{y}_i(k, \theta_n) \text{ and } \overline{r}_i(k) = \overline{\hat{y}_i}(k) - \hat{y}_i(k, \theta_n) \tag{24}$$

where $\underline{\hat{y}}_i(k)$ and $\overline{\hat{y}}_i(k)$ are the bounds of the system output estimation computed component-wise using the interval observer (14) and obtained according to (18).

Then, the fault detection test could be based on checking if the residuals satisfy or not the condition given by (23). In case that this condition does not hold, a fault can be indicated. Notice that checking condition (23) is equivalent to check condition (17).

Fault detection based on interval observers presents non detected faults (missed alarms) because of the uncertainty. This is due to the fact that there exists a minimum fault size that guarantees the activation of the fault detection test (23) despite the uncertainties. On the other hand, interval observers guarantee that there are no false alarms since uncertainty bounds are determined to explain the data collected in non-faulty scenarios for estimation.

4.2 Fault Isolation

Fault isolation consists in identifying the faults affecting the system. It is carried out on the basis of fault signatures, generated after the detection process, and their relation with all the considered faults. Robust residual evaluation presented in Section 4.1 allows obtaining a set of observed *fault signatures* $\phi(k) = [\phi_1(k), \phi_2(k), \ldots, \phi_{ny}(k)]$, where each fault indicator is given by:

$$\phi_i(k) = \begin{cases} 0 \text{ if } r_i(k) \in [\underline{r}_i(k) - \sigma_i, \overline{r}_i(k) + \sigma_i] \\ 1 \text{ if } r_i(k) \notin [\underline{r}_i(k) - \sigma_i, \overline{r}_i(k) + \sigma_i] \end{cases} \tag{25}$$

Standard fault isolation reasoning exploits the knowledge about the binary relation between the set of fault hypothesis and the set of residuals that is stored in the so called *Fault Signature Matrix* (FSM), denoted as M. An element $m_{i,j}$ (i indicates rows, j indicates columns) of M is equal to 1 if the fault f^j affects the computation of the residual r_i; otherwise, the element $m_{i,j}$ is zero-valued. A column of M is known as a *theoretical fault signature* and indicates which residuals are affected by a given fault. A set of faults is *isolable* if all the columns in M are different (two columns that are equal indicate two faults that can not be distinguished).

The procedure accepted as standard by the FDI community involves finding a matching between the observed fault signature and one of the theoretical fault signatures. However, this reasoning is not appropriate in an unknown but bounded context. Due to the uncertainty, when a fault is present in the system, an undefined number of the residuals affected by the fault can be found inconsistent, mainly depending on the sensitivity of each residual with respect to the fault and on the fault magnitude. In this case, if the column-matching procedure is used, then the particular fault will not be identified. An appropriate reasoning which comes from the DX community only consider the residuals that are inconsistent when searching for the fault (inconsistency is relevant, consistency is not). Based on the proposed framework by [Cordier et al., 2004], the fault signature matrix is interpreted as in DX approach to fault isolation considering separately each line corresponding to a violated ARR, (i.e., a set of components that are to be considered abnormal in order to be consistent with the observed fault signature) before searching for a common explanation, i.e., follows a row view of the fault signature matrix.

From the set of 10 faults proposed in the benchmark, the fault scenarios f_2, f_6 and f_{10} were not treated in this paper because it was not possible to find suitable models in the literature to perform model based diagnosis, remaining to be studied in future work.

Based on the information provided by the set of obtained residuals, the logical test that allows to isolate the faults has been generated. Tables 3 and 4 list the logical reasoning test in the case of applying column and row reasoning approaches respectively, where $\Delta \mathrm{N}r_i$ indicates an abnormal behavior of i^{th} residual.

5. SIMULATION RESULTS

In this section , the results obtained for some of the faults scenarios detailed in [Odgaard and Johnson, 2013], are presented. These faults are only present during a determined period of time. In the following section some representative results will be presented. In Figure 3, the fault scenario f_1 is presented, which corresponds to a blade root moment sensor scaled by a factor of 0.95 and it is present between 20 s and 45 s. On the other hand, Figure 4 presents fault scenario f_5, which occurs in the generator

Table 2. Fault Scenarios

No.	Faults	Type
f_1	Blade root bending moment sensor	Scaling
f_2	Accelerometer	Offset
f_3	Generator speed sensor	Scaling
f_4	Pitch angle sensor	Stuck
f_5	Generator power sensor	Scaling
f_6	Low speed shaft position encoder	Bit error
f_7	Pitch actuator	Abrupt
f_8	Pitch actuator	Slow
f_9	Torque offset	Offset
f_{10}	Yaw drive	Stuck drive

Table 3. Column reasoning approach

Logical Test	Diagnostic
$\Delta \mathrm{N}r_2$	$f_{1-M,B,1,m}$
$\Delta \mathrm{N}r_3$	$f_{1-M,B,2,m}$
$\Delta \mathrm{N}r_4$	$f_{1-M,B,3,m}$
$\Delta \mathrm{N}r_1 \wedge \Delta \mathrm{N}r_9 \wedge \Delta \mathrm{N}r_{11} \wedge \Delta \mathrm{N}r_{12}$	f_3
$\Delta \mathrm{N}r_2 \wedge \Delta \mathrm{N}r_6$	$f_{4-\beta 1} \vee f_{(7-8)-PA1}$
$\Delta \mathrm{N}r_3 \wedge \Delta \mathrm{N}r_7$	$f_{4-\beta 2} \vee f_{(7-8)-PA2}$
$\Delta \mathrm{N}r_4 \wedge \Delta \mathrm{N}r_8$	$f_{4-\beta 3} \vee f_{(7-8)-PA3}$
$\Delta \mathrm{N}r_1$	$f_3 \vee f_5 \vee f_9$
$\Delta \mathrm{N}r_1 \wedge \Delta \mathrm{N}r_5 \wedge \Delta \mathrm{N}r_9 \wedge \Delta \mathrm{N}r_{10} \wedge \Delta \mathrm{N}r_{11}$	$f_3 \vee f_9$

Table 4. Row reasoning approach

Logical Test	Diagnostic
$\Delta \mathrm{N}r_1$	$f_3 \vee f_5 \vee f_9$
$\Delta \mathrm{N}r_2$	$f_{1-M,B,1,m} \vee f_{4-\beta 1} \vee f_{7-PA1} \vee f_{8-PA1}$
$\Delta \mathrm{N}r_3$	$f_{1-M,B,2,m} \vee f_{4-\beta 2} \vee f_{7-PA2} \vee f_{8-PA2}$
$\Delta \mathrm{N}r_4$	$f_{1-M,B,3,m} \vee f_{4-\beta 3} \vee f_{7-PA3} \vee f_{8-PA3}$
$\Delta \mathrm{N}r_5$	f_9
$\Delta \mathrm{N}r_6$	$f_{4-\beta 1} \vee f_{7-PA1} \vee f_{8-PA1}$
$\Delta \mathrm{N}r_7$	$f_{4-\beta 2} \vee f_{7-PA2} \vee f_{8-PA2}$
$\Delta \mathrm{N}r_8$	$f_{4-\beta 3} \vee f_{7-PA3} \vee f_{8-PA3}$
$\Delta \mathrm{N}r_9$	$f_3 \vee f_9$
$\Delta \mathrm{N}r_{10}$	f_9
$\Delta \mathrm{N}r_{11}$	$f_3 \vee f_9$
$\Delta \mathrm{N}r_{12}$	f_3

power sensor scaled by a factor of 1.1. Fault f_5 is present in the time interval from 240s to 265s.

In both fault scenarios shown in Figures 3 and 4, it can be observed that the measurement goes out of the detection thresholds and that the fault indicator activates during the interval of time in which the fault is present, either permanently or intermittently. The fault detection results are summarized in Table 5. The values for required detection time (t_D) are those specified in the benchmark [Odgaard and Johnson, 2013]. The real time detection (t_D real) is the one obtained for the first residual activated in presence of the fault, where T_s is the sampling period. It is also shown which residuals were activated for each one of the considered fault scenarios during the simulation tests.

In the work of [Blesa et al., 2013] interval based observers have also been applied for fault diagnosis of the first benchmark [Odgaard and Stoustrup, 2013], one difference between the benchmark solution of [Blesa et al., 2013] and this one relies in the residual generation. The residual generation in [Blesa et al., 2013] relies on physical redundancy, there are two measurements for the pitch systems of all blades, the rotor and the generator. Instead, the FDI scheme presented in this paper is strictly model

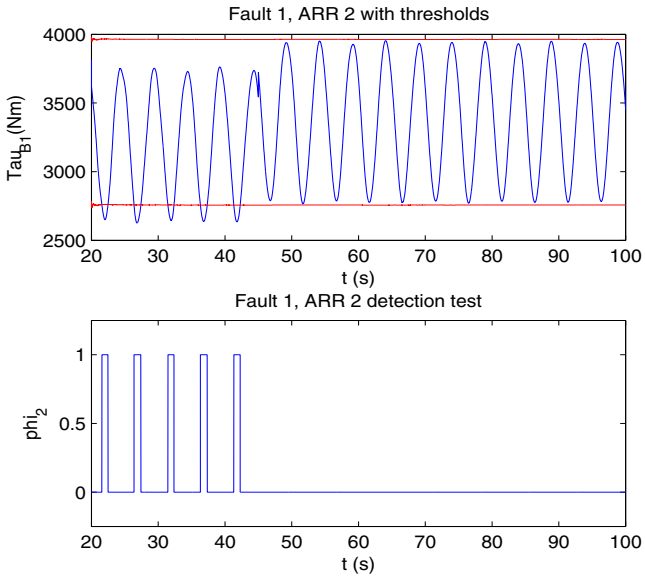

Fig. 3. Fault scenario f_1: (up) measurement and detection thresholds and (down) fault indicator

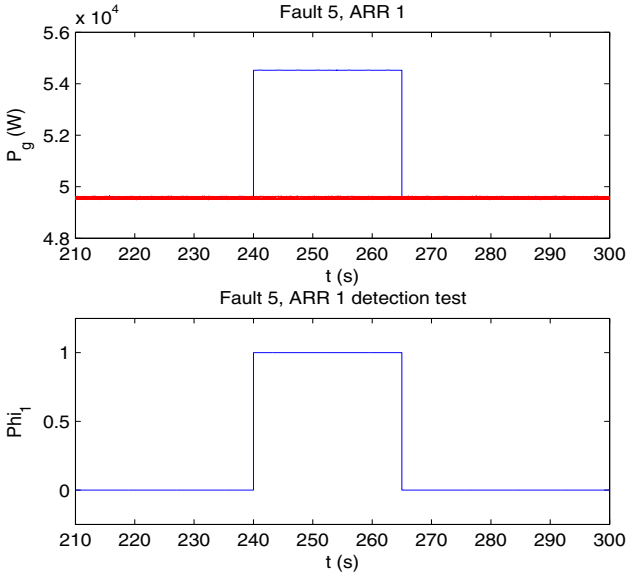

Fig. 4. Fault scenario f_5: (up) measurement and detection thresholds and (down) fault indicator

Table 5. Fault Detection Results

Fault	t_D required	t_D real	Activated Residuals
f_1	<10 T_s	128 T_s	r_2, r_3 and r_4
f_2	*Not considered*	-	-
f_3	<10 T_s	3 T_s	r_1, r_9 and r_12
f_4	<10 T_s	3 T_s	r_2, r_3, r_4, r_6, r_7 and r_8
f_5	<10 T_s	3 T_s	r_1
f_6	*Not considered*	-	-
f_7	<8 T_s	375 T_s	r_2, r_3 and r_4
f_8	<100 T_s	33 T_s	r_2, r_3 and r_4
f_9	<3 T_s	3 T_s	r_5 and r_9
f_{10}	*Not considered*	-	-

based in which all the residuals are generated using the structural relations derived from the physical models. Both

FDI schemes presented good performance regarding the detection and isolation requirements.

5.1 Isolation based on Column Reasoning

Comparing the activated residuals with the logic conditions described in Table 3 it is observed that faults f_1 and f_5 can be isolated. Faults 4, 7 and 8 correspond to faults that occur in the sensors and actuators of the pitch subsystems, they have the same fault signature, as a consequence they cannot be isolated between each other. Faults 3 and 9 signatures do not match exactly with its theoretical ones because not all its residuals were activated, see Table 5. Therefore in a strict reasoning, these faults scenarios are not isolable because do not match with none of the signatures in the theoretical signature matrix. However, in the case these fault scenarios occur it is possible to calculate which one of fault signatures is the one that adjust the best to the current observation.

5.2 Isolation based on Row Reasoning

Comparing the activated residuals with the logic conditions described in Table (4), the following diagnosis is obtained. In the case of activation of r_1, the possible faults would be f_3, f_5 or f_9. In the case of r_2 or r_6 activation, the fault would be $f_{4-\beta 1} \vee f_{7-PA1} \vee f_{8-PA1}$, detecting a fault in pitch subsystem 1 but not being able to isolate if it is the sensor or the actuator the faulty component. The same diagnosis is obtained in case that r_3 or r_7 and r_4 or r_8 activates, the fault would be in pitch subsystem 2 or 3 either the sensor or the actuator. If r_5 activates, fault 9 would be isolated. In the case of r_9 activation, the possible faults would be f_3 or f_9. The case of r_{10} activation would result in f_9 isolation. If r_{12} activates, the isolated fault would be f_3.

6. CONCLUSIONS

In this work, a model based diagnosis approach using interval based ARRs (static and dynamic) and observers has been applied to an advanced wind turbine benchmark, in which a set of fault scenarios was defined. In most of the cases, the obtained ARRs proved to be able to detect the different fault scenarios of different types (scaling, offset and stuck) taken into account the uncertainty in the models parameters and the noise in the sensors proposed in the benchmark. The quality of the models used for fault detection is of primary importance. In case that theoretical models do not present a good approximation of the observed dynamics, an experimental model can be used if it is correctly calibrated.

The fault isolation techniques based on column and row reasoning applied to the signature matrix obtained from the simulation tests, have shown that only some of the faults were completely isolable. The limitation of column reasoning is that in case that not all the residuals activate, a none exact match with theoretical FSM is obtained and therefore the isolation is not very robust. Instead, the DX row based reasoning is more robust since it allows to isolate faults even though not all the theoretical residuals activate. As final conclusion, to improve the obtained results, it is necessary to add more ARRs that lead to a more complete fault signature matrix in order to improve isolation and robustness.

ACKNOWLEDGEMENTS

This work has been funded by the Spanish MINECO through the project CYCYT SHERECS (ref. DPI2011-26243) and by AGAUR Doctorat Industrial 2013-DI-041.

REFERENCES

M. Blanke, M. Kinnaert, J. Lunze and M. Staroswiecki. Diagnosis and Fault-Tolerant Control. *Springer-Verlag Berlin Heidelberg*, 2006

J. Blesa, F. Nejjari, D. Rotondo and V. Puig. Robust Fault Detection and Isolation of Wind Turbines using Interval Observers *Conference on Control and Fault-Tolerant Systems (SysTol)*, October 9-11,2013. Nice, France

M.O. Cordier,P. Dague, F. Lévy, J. Montmain, M. Staroswiecki and L. Travéé-Massuyès. Conflicts Versus Analytical Redundancy Relations: A Comparative Analysis of the Model Based Diagnosis Approach From the Artificial Intelligence and Automatic Control Perspectives *IEEE Transactions on Systems, Man, and Cybernetics - Part B: Cybernetics*, volume 34, pages 2163–2177, 2004

M. Chilali and P. Gahinet. Design with pole placement constraints: an LMI approach. *IEEE Transactions on Automatic Control*, volume 41, pages 358–367, 1996

T. Esbensen and C. Sloth. Fault Diagnosis and Fault-Tolerant Control of Wind Turbines. *Master Thesis, Aalborg University*, 2009.

J. Jonkman and M.L. Buhl. Fast User's Guide *National Renewal Energy Laboratory Techical Report, USA*, August 2005

H. Markou, T. Buhl, B. Marrant and T.G van Engelen. Morphological Study of Aeroelastic Control Concepts for Wind Turbines. *Report of the European Union project STABCON*, 2002.

M. Milanese, J. Norton, H. Piet-Lahanier and É. Walter (Eds.) Bounding Approaches to System Identification. *Springer*, 1996

P. Odgaard and J. Stoustrup. Fault-Tolerant Control of Wind Turbines: A Benchmark Model *IEEE Transactions on Control Systems Technology*, Vol. 21, 4, pages 1168–1182, 2013

P. Odgaard and K. Johnson. Wind turbine fault detection and fault tolerant control - an enhanced benchmark challenge. *Proceedings of the American Control Conference*, pages 4447–4452, 2013.

V. Puig, J. Saludes and J. Quevedo. Worst-Case Simulation of Discrete Linear Time-Invariant Interval Dynamic Systems *Reliable Computing*, pages 251–290, 2003

V. Puig, A. Stancu, T. Escobet, F. Nejjari, J. Quevedo, and R. J. Patton. Passive Robust Fault Detection using Interval Observers: Application to the DAMADICS Benchmark Problem. *Control Engineering Practice*, volume 14, issue 6, pages 621-633, 2006

V. Puig, S. Montes and J. Blesa. Adaptive threshold generation in robust fault detection using interval models: time-domain and frequency-domain approaches *International Journal of Adaptive Control and Signal Processing*, volume 27, issue 10, pages 873-901, 2013